



OPEN

# A fluorometric assay to determine labile copper(II) ions in serum

Maria Maares<sup>1,2</sup>, Alessia Haupt<sup>1</sup>, Christoph Schüßler<sup>1,2</sup>, Marcel Kulike-Koczula<sup>3</sup>, Julian Hackler<sup>2,4</sup>, Claudia Keil<sup>1</sup>, Isabelle Mohr<sup>5</sup>, Lutz Schomburg<sup>2,4</sup>, Roderich D. Süssmuth<sup>3</sup>, Hans Zischka<sup>6,7</sup>, Uta Merle<sup>5</sup> & Hajo Haase<sup>1,2</sup>✉

Labile copper(II) ions ( $\text{Cu}^{2+}$ ) in serum are considered to be readily available for cellular uptake and to constitute the biologically active  $\text{Cu}^{2+}$  species in the blood. It might also be suitable to reflect copper dyshomeostasis during diseases such as Wilson's disease (WD) or neurological disorders. So far, no direct quantification method has been described to determine this small  $\text{Cu}^{2+}$  subset. This study introduces a fluorometric high throughput assay using the novel  $\text{Cu}^{2+}$  binding fluoresceine-peptide sensor FP4 (Kd of the  $\text{Cu}^{2+}$ -FP4-complex 0.38 pM) to determine labile  $\text{Cu}^{2+}$  in human and rat serum. Using 96 human serum samples, labile  $\text{Cu}^{2+}$  was measured to be  $0.14 \pm 0.05$  pM, showing no correlation with age or other serum trace elements. No sex-specific differences in labile  $\text{Cu}^{2+}$  concentrations were noted, in contrast to the total copper levels in serum. Analysis of the effect of drug therapy on labile  $\text{Cu}^{2+}$  in the sera of 19 patients with WD showed a significant decrease in labile  $\text{Cu}^{2+}$  following copper chelation therapy, suggesting that labile  $\text{Cu}^{2+}$  may be a specific marker of disease status and that the assay could be suitable for monitoring treatment progress.

The essential trace element copper is indispensable for various physiological functions, such as support of oxidative phosphorylation, antioxidant activity, formation of several hormones, and iron metabolism<sup>1,2</sup>. The metal is distributed throughout the body via the bloodstream, and 0.75–1.4 mg/L  $\text{Cu}^{2+}$  can be found in human serum<sup>3,4</sup>. Approximately 70–90% thereof is contained in ceruloplasmin (CP), while the remaining  $\text{Cu}^{2+}$ , which is typically being referred to as loosely bound  $\text{Cu}^{2+}$ , is associated with albumin (10–15%),  $\alpha$ -macroglobulin (5–15%), clotting factors, enzymes (superoxide dismutase (SOD), Oxidases), metallothionein, as well as small  $\text{Cu}^{2+}$  carriers<sup>3–5</sup>. The loosely bound  $\text{Cu}^{2+}$  species comprises the whole amount of serum  $\text{Cu}^{2+}$  that is not bound to CP, whereas so-called labile  $\text{Cu}^{2+}$  represents a smaller subset of the loosely bound pool and is defined only to be in equilibrium with low molecular weight (LMW) ligands, e.g., amino acids. This labile  $\text{Cu}^{2+}$  pool is considered to be readily available for cellular uptake and was even discussed to cross the blood–brain barrier as LMW- $\text{Cu}^{2+}$ -complexes<sup>6</sup>. As copper is redox active, an increase of labile  $\text{Cu}^{2+}$  must be tightly controlled to prevent formation of reactive oxygen species and tissue damage<sup>1,7</sup>.

Diseases associated with copper dishomeostasis and changes in serum  $\text{Cu}^{2+}$  are Menkes, Wilson's (WD)<sup>8,9</sup>, cancer<sup>10</sup>, and neurodegenerative diseases<sup>1,11–16</sup>, such as Parkinson's and Alzheimer's disease. Particularly in the copper storage disorder WD<sup>8,9</sup> and neurodegenerative diseases<sup>1,11–13,15</sup> both loosely bound and labile levels of serum  $\text{Cu}^{2+}$  were found to be elevated. Hence, these serum  $\text{Cu}^{2+}$  species are considered to serve as promising diagnostic markers for disease-related alterations of copper homeostasis<sup>6,13</sup>.

In addition to indirect quantification of loosely bound or non-CP-bound  $\text{Cu}^{2+}$  in serum by determination of CP content and total  $\text{Cu}^{2+}$  content<sup>15,17,18</sup>, several experimental approaches for direct measurement of this  $\text{Cu}^{2+}$  species have been developed to date. This  $\text{Cu}^{2+}$  pool, which is also often defined as extractable or exchangeable  $\text{Cu}^{2+}$ , has been either directly quantified by liquid chromatography (LC) coupled to inductively coupled plasma-mass spectrometry (ICP-MS)<sup>19,20</sup>, or after extracting the loosely bound metal in serum with  $\text{Cu}^{2+}$  chelators such as EDTA<sup>9,21</sup> or  $\text{Cu}^{2+}$ -affine resins<sup>22,23</sup> followed by size ultrafiltration or size exclusion chromatography (SEC)

<sup>1</sup>Department of Food Chemistry and Toxicology, Technische Universität Berlin, Straße des 17. Juni 135, 10623 Berlin, Germany. <sup>2</sup>TraceAge-DFG Research Unit on Interactions of Essential Trace Elements in Healthy and Diseased Elderly, Potsdam-Berlin-Jena, Germany. <sup>3</sup>Department of Organic and Biological Chemistry, Technische Universität Berlin, Straße des 17. Juni 135, 10623 Berlin, Germany. <sup>4</sup>Institute for Experimental Endocrinology, Berlin Institute of Health, Charité-Universitätsmedizin Berlin, Corporate Member of Freie Universität Berlin, Humboldt-Universität zu Berlin, 10115 Berlin, Germany. <sup>5</sup>Department of Internal Medicine IV, University Hospital Heidelberg, 69120 Heidelberg, Germany. <sup>6</sup>Institute of Molecular Toxicology and Pharmacology, Helmholtz Center Munich, German Research Center for Environmental Health, Ingolstaedter Landstrasse 1, 85764 Neuherberg, Germany. <sup>7</sup>School of Medicine, Institute of Toxicology and Environmental Hygiene, Technical University Munich, Biedersteiner Strasse 29, 80802 Munich, Germany. ✉email: haase@tu-berlin.de

and quantified either by ICP-MS<sup>21–23</sup>, atomic absorption spectrometry (AAS)<sup>9,23</sup>, or fluorescent Cu<sup>2+</sup> sensors<sup>13</sup>. The resulting concentration of loosely bound Cu<sup>2+</sup> was in the range of 0.5–7 μM<sup>9,13,19–23</sup>. Up to now, the smaller serum Cu<sup>2+</sup> fraction that is not bound to CP or albumin, but in equilibrium with the remainder of Cu<sup>2+</sup> binding compounds in serum, was quantified by means of ultrafiltration followed by direct measurement of copper by AAS<sup>6,24,25</sup> or ICP-MS<sup>8</sup>. This fraction is in the nanomolar concentration range<sup>6</sup> and has often been equated with labile Cu<sup>2+</sup>. However, there is at present no suitable method allowing direct quantification of labile Cu<sup>2+</sup> in serum without a prior extraction step. The use of metal-responsive fluorescent sensors to quantify free metal species in biofluids represents a suitable approach to directly measure metal cations in serum while requiring small sample volumes<sup>26</sup>. Therefore, the aim of this study was to establish a fluorescence-based method for determining the concentration of labile Cu<sup>2+</sup> in serum samples with a small sample volume and a high throughput.

## Materials and methods

### Materials

Chelex<sup>®</sup> 100 resin (Bio-Rad, Hercules, USA), CuSO<sub>4</sub>, Dimethylsulfoxide (DMSO), Ethylenediaminetetraacetic acid (EDTA), Ethylene glycol bis(2-aminoethyl ether)tetraacetic acid (EGTA), 4-(2-hydroxyethyl)-1-piperazineethanesulfonic acid (HEPES), histidine, were purchased from Sigma Aldrich (Munich, Germany). All other materials were from standard sources and of analytical purity.

### Fluorescent sensors

Fluorescein peptide 4 (FP4) was synthesized by Peptide Specialty Laboratories GmbH (Heidelberg, Germany). Dansyl peptide 4 (DP4) was synthesized by manual solid phase peptide synthesis (SPPS) using a standard Fmoc-strategy. Fmoc-K(DNS)-OH was used as starting material for the SPPS and synthesized according to the method of Williamson et al.<sup>27</sup> (for details refer to Supplementary Sect. 1). Stock solutions of FP4 and DP4 (1 mM, in DMSO) were aliquoted and stored at –20 °C. Each aliquot was thawed only twice.

### Determination of Cu<sup>2+</sup> binding affinity

Determination of the dissociation constant of the Cu<sup>2+</sup>-FP4-complex was done as described<sup>28,29</sup> using histidine and EGTA as competitors for Cu<sup>2+</sup> binding. Experiments were performed in assay buffer, consisting of 50 mM HEPES, pH 7.4, depleted from bivalent metal ions by treatment with Chelex<sup>®</sup> 100 resin<sup>26</sup>. To determine the aqueous Cu<sup>2+</sup> concentration, CHEAQS Next 2014–2020 software and the NIST Database 46 Version 8.0 was applied, using log K<sub>A</sub> for Cu<sup>2+</sup>-histidine, Cu<sup>2+</sup>-histidine<sub>2</sub>, and Cu<sup>2+</sup>-EGTA at pH 7.4 from Young et al.<sup>28</sup> and log K<sub>A</sub> for Cu<sup>2+</sup>-HEPES from Sokolowska et al.<sup>30</sup> (Supplementary Table 1).

### Human serum samples

A commercially available standard serum derived from a mixture of human serum samples was used as reference serum (in.vent Diagnostica GmbH, Hennigsdorf, Germany). A set of commercially available individual human serum samples (N = 96, Table 1) (in.vent Diagnostica GmbH, Hennigsdorf, Germany) served as a reference cohort for healthy individuals within this study.

Serum samples of WD patients were obtained from 19 patients (Table 1) at the time point of disease diagnosis and from the same patients after initiation of medical treatment. Mean treatment duration till second time point under therapy was 72.9 (range 6–144) months. Patients were recruited between 2010 and 2018 at the University Hospital Heidelberg, Germany, as part of the clinical trial 'Biochemical and genetic markers of liver diseases'. Clinical parameters of the investigated human WD patients and the respective medical treatment are listed in Supplementary Tables 2 and 3. The study was approved by the ethics committee of the University of Heidelberg and informed consent to participate in the study was obtained from each subject. The study was carried out in accordance with the Declaration of Helsinki.

### Rat serum samples

Control Atp7b+/- LPP rats (N = 5; crossbreed between Long Evans cinnamon rats and Piebald Virol Glaxo rats) were fed ad libitum with standard rat chow (Altromin Spezialfutter GmbH, Seelenskamp, Germany) and tap water<sup>31</sup>. At the age of 81–93 days, animals were sacrificed, and serum was collected. Experiments were approved by the government authorities of the Regierung von Oberbayern, Munich, Germany. Animals were maintained under the Guidelines for the Care and Use of Laboratory Animals of the Helmholtz Center Munich. All methods are reported in accordance with ARRIVE guidelines.

	Female	Male
Human control cohort (N = 96)		
Number of donors	60 (62.5%)	36 (37.5%)
Age (median, IQR)	35.0 (24.0; 43.8)	33.5 (26.3; 47.5)
Wilson disease patients (N = 19)		
Number of donors	9 (47.4%)	10 (52.6%)
Age (median, IQR)	23 (19; 30)	28 (21.3; 33)

**Table 1.** Overview of human serum samples in this study. IQR interquartile range.

### Labile serum Cu<sup>2+</sup>

Similar to the labile zinc (Zn<sup>2+</sup>) assay reported by Alker et al.<sup>26</sup>, 50 mM HEPES buffer, pH 7.4, bivalent metal ion-depleted with Chelex® 100 resin, was used in all steps. 20 µL human or rat serum, pre-diluted to 5% in ice-cold assay buffer, were added to 10 nM FP4 in 80 µL assay buffer in black 96-well plates (Brand, Wertheim, Germany) and gently shaken in the dark. During the assay, only the inner 60 wells were used, and each sample was analyzed in triplicates. The outer wells were filled with distilled water to ensure a uniform temperature over the entire plate. After 60 min, the fluorescence signal (F) of FP4 was measured using a SPARK Tecan plate reader (Tecan, Switzerland) at  $\lambda_{\text{ex}} = 495$  nm and  $\lambda_{\text{em}} = 523$  nm. Subsequently, 5 µL of 42 mM EDTA (diluted in assay buffer) was added to the wells, resulting in a final concentration of 2 mM EDTA, and incubated for additional 60 min. After measuring the maximum fluorescence signal of the sensor without any bound Cu<sup>2+</sup> (F<sub>apo</sub>), the minimum fluorescence signal (F<sub>Cu</sub>) was generated by adding 5 µL of 48.4 mM CuSO<sub>4</sub> (in distilled water), corresponding to a final Cu<sup>2+</sup> concentration of 2.2 mM, and the fluorescence intensity was determined after incubation for further 60 min. All steps were performed in the dark and at room temperature (25 °C). The labile Cu<sup>2+</sup> concentration was calculated according to Gryniewicz et al.<sup>32</sup> by multiplying  $[(F_{\text{apo}} - F)/(F - F_{\text{Cu}})]$  with the dissociation constant of the Cu<sup>2+</sup>-FP4-complex of 0.38 pM, determined in this study.

### Total trace element levels in serum

Concentrations of total selenium, copper, and zinc in the serum samples were quantified with total reflection X-ray fluorescence (TXRF) using a benchtop TXRF spectrometer (S4 T-STAR, Bruker Nano GmbH, Berlin, Germany) as previously described<sup>33,34</sup>.

### Labile serum Zn<sup>2+</sup>

The concentration of labile Zn<sup>2+</sup> was determined by a fluorometric method using the low molecular weight Zn<sup>2+</sup> sensor Zinpyr-1 (Santa Cruz biotechnology, Dallas, USA) as described<sup>26</sup>.

### Statistical analysis

Statistical analysis was performed using GraphPad Prism software version 9.3.1 (GraphPad Software Inc., San Diego, CA, USA). Data were tested for normal distribution using the Shapiro–Wilk test. Correlations were analyzed using Spearman correlation analysis. Statistically significant differences between two means were identified with t-test for parametric or Mann–Whitney test for non-parametric data, or between three or more means by one-way analysis of variance (ANOVA) followed by Tukey's multiple post hoc comparison test or non-parametric Kruskal–Wallis with Dunn's multiple comparison test. Differences were considered significant if p values were \* $p < 0.05$ , \*\* $p < 0.01$ , or \*\*\* $p < 0.001$ , as indicated in the figure legends. Error bars represent standard deviation (SD) of at least three independent experiments.

## Results and discussion

### Choice of Cu<sup>2+</sup>-responsive fluorescent sensor

A metal-responsive sensor for the detection and quantification of labile Cu<sup>2+</sup> in serum must exhibit Cu<sup>2+</sup>-dependent fluorescence changes, high Cu<sup>2+</sup>-selectivity and -sensitivity, but also have suitable Cu<sup>2+</sup> affinity and reversible binding of the metal<sup>35</sup>. In addition, good water solubility and negligible interaction with the complex biomatrix are required for the application of such sensors in biofluids, such as serum containing proteins, lipids, and carbohydrates. A suitable fluorescence yield ( $\Phi$ ) and extinction coefficient ( $\epsilon$ ), which defines the brightness of the fluorophore =  $\Phi * \epsilon$ <sup>35,36</sup> is another crucial requirement for the physicochemical properties of sensors. Initially, the peptide-based dansyl Cu<sup>2+</sup> sensors developed by Young et al. were chosen as they seemed to meet all prerequisites<sup>28</sup>. Unfortunately, DP4 (Fig. 1a) turned out to be poorly suited for detecting labile Cu<sup>2+</sup> in serum samples, as the absorption of serum proteins interfered with fluorescence of the dansyl sensor. According to the excitation and emission spectra of DP4 in the presence of 1% HS or correspondingly diluted physiological serum albumin levels, added as 0.5 g/L bovine serum albumin (BSA), this was mainly due to the albumin content of serum (Fig. 1b, c). To circumvent this interference, the dansyl fluorophore of the peptide sensor was replaced with carboxyfluorescein (FAM), which emits light of lower energy and has a higher fluorescence yield and extinction coefficient than the dansyl molecule<sup>28,37</sup>, leading to the sensor FP4 (Fig. 1d). In contrast to DP4, FP4 was undisturbed by any autofluorescence or absorbance of serum proteins. Comparison of FP4 in the presence and absence of HS shows that the emission and excitation spectra were not affected by the presence of serum (Fig. 1e, f). Furthermore, the metal selectivity of the probe was assessed (Supplementary Fig. 1). No physiologically relevant cation in serum had an effect on sensor fluorescence or Cu<sup>2+</sup> binding by FP4. However, FP4 fluorescence was quenched by adding a 20-fold excess of Ni<sup>2+</sup> to FP4, yet the applied concentrations do not represent physiological nickel levels in serum<sup>38</sup>. Furthermore, subsequent addition of Cu<sup>2+</sup> resulted in a decrease in fluorescence comparable to that observed with FP4 and Cu<sup>2+</sup> alone.

### Dissociation constant of the Cu<sup>2+</sup>-FP4-complex

To assess whether introduction of FAM did influence the Cu<sup>2+</sup>-affinity of the probe, the dissociation constant of FP4 was determined with EGTA and histidine by a similar experimental approach as the one applied by Young et al.<sup>28</sup>, yielding a conditional  $\log(\text{Kd}) = -12.416$  for the Cu<sup>2+</sup>-FP4-complex, corresponding to 0.38 pM (Fig. 2, Supplementary Table 1). Accordingly, the Cu<sup>2+</sup>-affinity of FP4 is lower than that of DP4, but in the vicinity of the hitherto reported labile Cu<sup>2+</sup> levels in serum<sup>6,22</sup> and thus suitable for determining this Cu<sup>2+</sup> species.

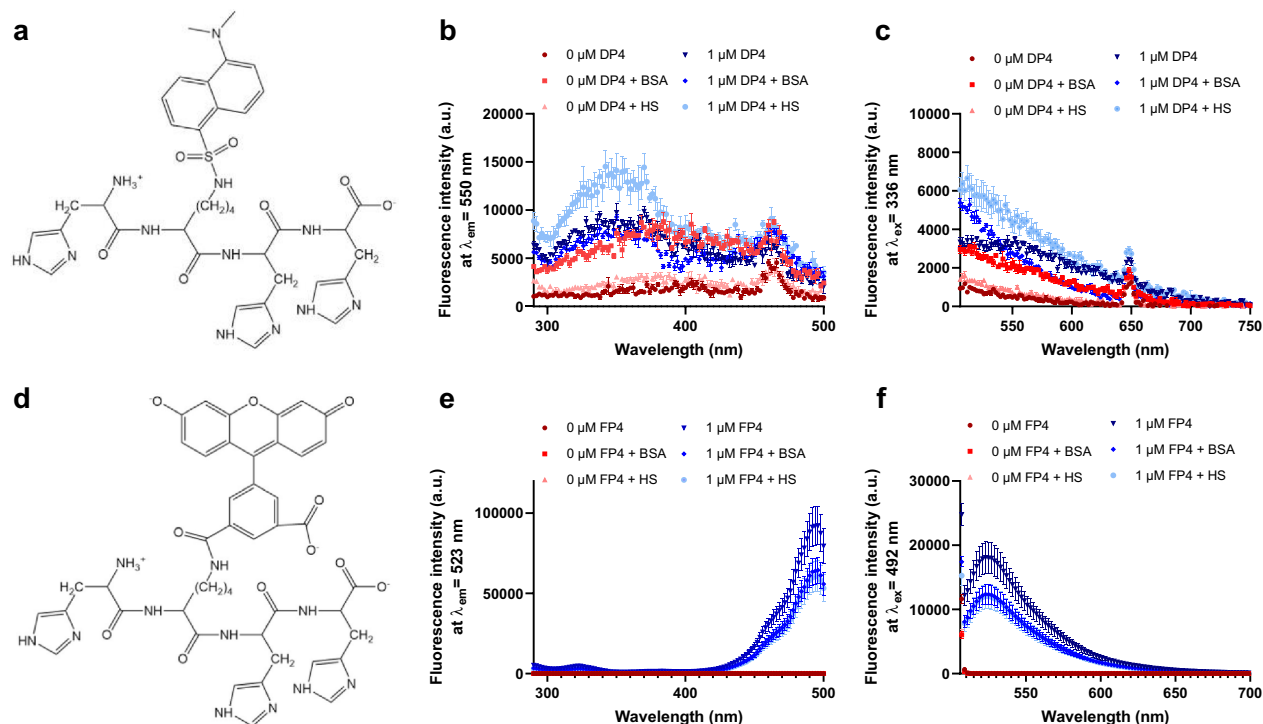


**Figure 1.** Spectra of DP4 and FP4. Chemical structure, excitation, and emission spectra of 1  $\mu\text{M}$  DP4 (a–c) and 1  $\mu\text{M}$  FP4 (d–f) in 50 mM HEPES with 1% human serum or 2.5 mg/mL BSA (final concentrations). Data are shown as means  $\pm$  SD of three independent experiments.

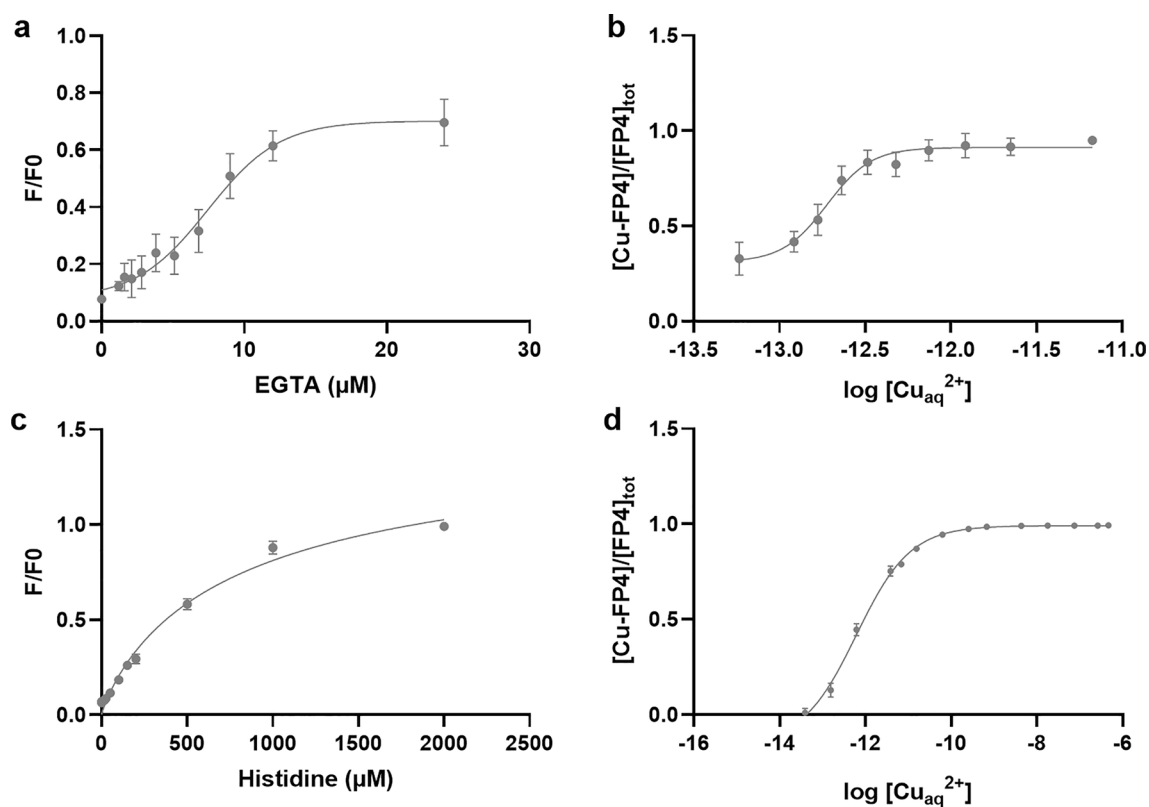


**Figure 2.**  $\text{Cu}^{2+}$  binding affinity of FP4. Relative fluorescence of FP4 in the presence of different concentrations of EGTA (a) and histidine (c). Sigmoidal dose response of  $[\text{Cu-FP4}]/[\text{FP4}]_{\text{tot}}$  and the labile  $\text{Cu}^{2+}$  concentration  $\log [\text{Cu}_{\text{aq}}^{2+}]$  upon titration with chelators EGTA (b) or histidine (d). Shown are means  $\pm$  standard deviation of three independent experiments.

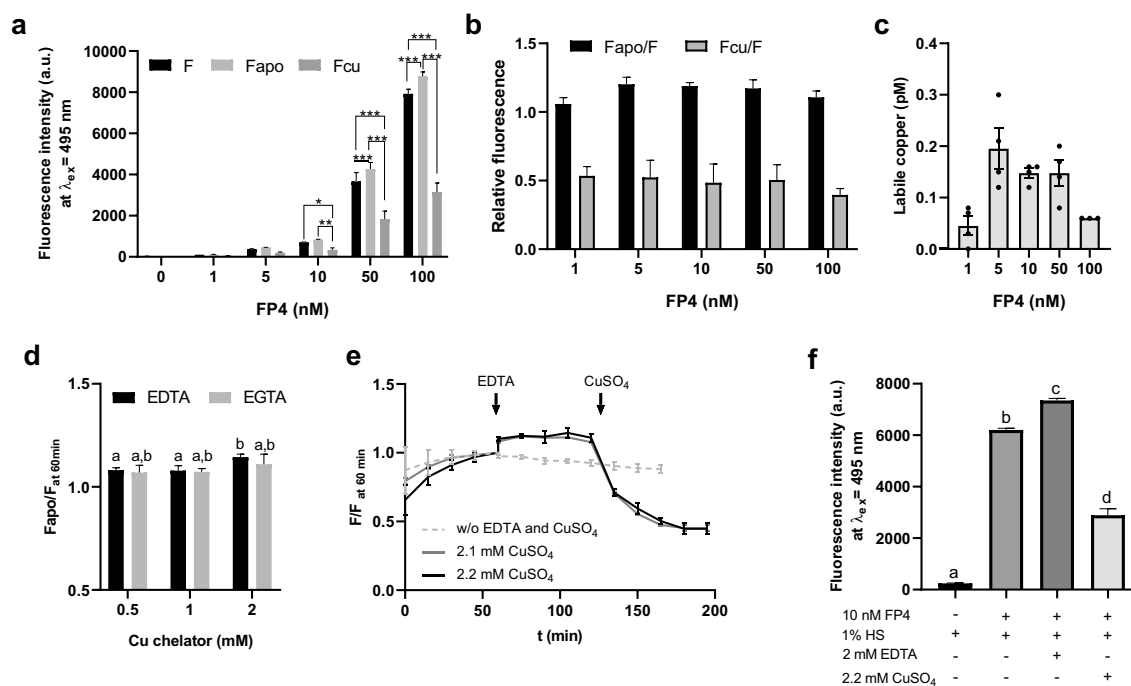


**Figure 3.** Optimization of assay parameters. Assay parameters were tested in the presence of 1% human reference serum. **(a)** Fluorescence intensity depending on sensor concentration (F), after the addition of 2 mM EDTA ( $F_{apo}$ ) and 2.2 mM  $CuSO_4$  ( $F_{cu}$ ). **(b)**  $F_{apo}/F$  and  $F_{cu}/F$  ratios of 1–100 nM FP4 in the presence of 1% HS. **(c)** Labile  $Cu^{2+}$  (pM) in HS depending on sensor concentration. **(d)** Fluorescence of apo-FP4 in the presence of 1% HS as ratios of the maximal fluorescence upon addition of 0.5–2 mM EDTA or EGTA relative to the FP4 fluorescence at 60 min. **(e)** Time course of the fluorescence signal of FP4 in 1% HS for parameters F,  $F_{apo}$  (after addition of 2 mM EDTA), and  $F_{cu}$  (after addition of 2.1 mM or 2.2 mM  $CuSO_4$ ) relative to the fluorescence at  $t = 60$  min. **(f)** Fluorescence of final parameters. Significant differences are indicated by \* $p < 0.05$ ; \* $p < 0.01$ ; \*\*\* $p < 0.001$  (a) (two way ANOVA with Sidak's multiple comparisons test) or by letters (d,f), whereas bars sharing a letter are not significantly different (one way ANOVA with Tukey's multiple comparisons test). Results are shown as means  $\pm$  SEM/SD of at least three independent experiments.

### Assay parameters

To minimize the perturbation of the equilibria between labile and bound  $Cu^{2+}$  in serum by the addition of another  $Cu^{2+}$  binding species added in form of the sensor, the probe concentration needs to be as low as possible<sup>26</sup>. To identify suitable concentrations of FP4, 0–100 nM FP4 were titrated to 1% human serum and baseline fluorescence (F) was measured, followed by detection of sensor fluorescence upon sequential addition of 2 mM EDTA as  $Cu^{2+}$  chelator and 2.2 mM  $Cu^{2+}$  to saturate the probe, generating  $F_{apo}$  and  $F_{cu}$ , respectively (Fig. 3). 10 nM FP4 were sufficient to induce a stable fluorescence signal distinguishable from the autofluorescence of serum and buffer (Fig. 3a) while providing maximum  $F_{apo}$  to F ratio (Fig. 3b). By determining the fractional saturation of the sensor in the presence of human serum and using the  $K_d$  for the  $Cu^{2+}$ -FP4-complex of 0.38 pM, the labile  $Cu^{2+}$  level in the reference serum was  $0.14 \pm 0.02$  pM when applying 10 nM sensor (Fig. 3c). The addition of 5–50 nM sensor had no effect on the calculated labile  $Cu^{2+}$  concentration, while the addition of excessive amounts of sensor (100 nM) considerably decreased the determined labile  $Cu^{2+}$  values (Fig. 3c). This confirms the importance of an optimized sensor concentration and is consistent with other studies on the influence of excessive sensor levels on the determined labile metal concentrations<sup>39,40</sup>.

After a suitable sensor concentration was found, the assay parameters F,  $F_{apo}$ , and  $F_{cu}$  had to be optimized with regard to incubation time and concentrations of  $Cu^{2+}$  and  $Cu^{2+}$  chelator, respectively. Comparison of the  $Cu^{2+}$  chelators EGTA and EDTA to measure the maximum fluorescence signal of the  $Cu^{2+}$ -free sensor ( $F_{apo}$ ) shows that 2 mM EDTA induced significantly higher fluorescence than lower EDTA concentrations, while no significant differences between the chelators and tested EGTA concentrations were observed. Accordingly, a final EDTA concentration of 2 mM was chosen to generate the  $F_{apo}$  signal in the final assay (Fig. 3d). After inducing  $F_{apo}$ , the addition of  $CuSO_4$  in excess (concentration per well: 2.2 mM) was required to fully saturate FP4 with  $Cu^{2+}$  and quench its fluorescence to yield the minimum fluorescence of the sensor ( $F_{cu}$ ) (Fig. 3e). In order to optimize the incubation time required to generate the assay parameters F,  $F_{apo}$ , and  $F_{cu}$ , time-resolved measurements were carried out, showing that an incubation of 60 min each were sufficient to allow establishing an equilibrium for  $Cu^{2+}$  in the distribution between the ligands in serum and FP4, generating stable fluorescence signals for all three parameters in human (Fig. 3e) and rat serum (Supplementary Fig. 2).

According to the final assay protocol, the assay time is about 3 h for up to 19 samples per plate and with parallel and slightly staggered preparation of 4 plates, a total of 76 samples can be analyzed within 4 h. Each



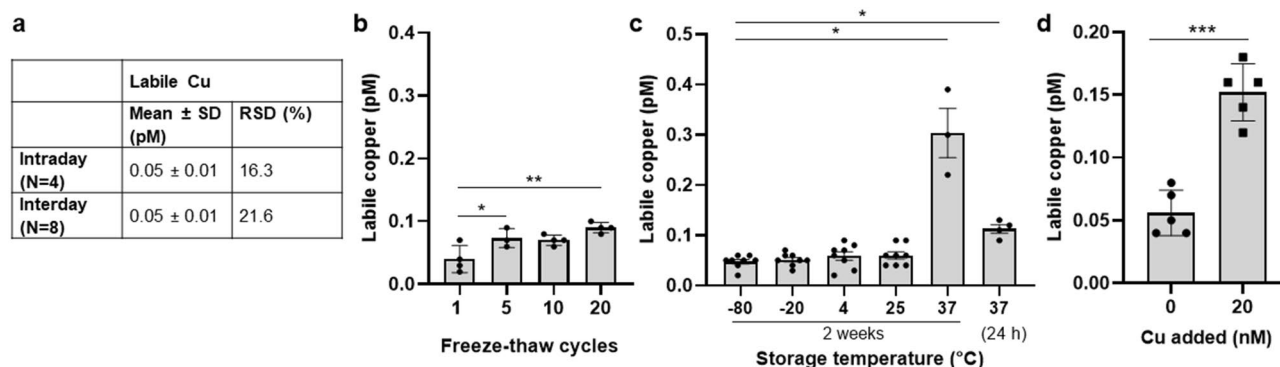


**Figure 4.** Stability of labile  $\text{Cu}^{2+}$  in serum. Repeatability and reproducibility of the assay are shown, including relative standard deviation (RSD) (a). Labile  $\text{Cu}^{2+}$  concentration in the reference serum depending on the number of freeze–thaw cycles (b) and storage temperature (c) are depicted. The labile  $\text{Cu}^{2+}$  concentration in 1% human reference serum upon spiking with 0 or 20 nM  $\text{CuSO}_4$  (N=4) is presented (d). Statistically significant differences between labile  $\text{Cu}^{2+}$  values were determined with non-parametric Kruskal–Wallis with Dunn’s multiple comparison test (b), ordinary one way ANOVA followed by Tukey multiple comparison test (c), and unpaired t-test ( $*p < 0.05$ ,  $**p < 0.01$ ;  $***p < 0.001$ ). Results are presented as data points including mean  $\pm$  SD of at least three independent experiments.

serum is tested in triplicate, which, including calculated dead volume, means a total sample volume requirement of only 5  $\mu\text{L}$  serum. A human reference serum is carried on each plate as quality control. The intra- and inter-day reproducibility of the assay was investigated by measuring the human reference serum, with a labile  $\text{Cu}^{2+}$  level of 0.05 pM, and evaluated with a relative standard deviation of 16.3% (intra-day) and 21.6% (inter-day) of the determined labile  $\text{Cu}^{2+}$  levels, respectively (Fig. 4a). To also characterize the requirements of the assay with regard to sample quality, the influences of freeze–thawing cycles, storage temperature, and  $\text{Cu}^{2+}$  spiking of the reference serum on the final labile  $\text{Cu}^{2+}$  concentration were determined (Fig. 4b–d). Accordingly, storage of samples at  $-80^\circ\text{C}$  or  $-20^\circ\text{C}$  is required (Fig. 4b) while only a minimum number of freeze–thaw cycles are acceptable (Fig. 4c) to avoid affecting the labile  $\text{Cu}^{2+}$  content in serum. In addition, the test can also be used to determine the labile  $\text{Cu}^{2+}$  content in serum from other species, such as rat serum, where a labile  $\text{Cu}^{2+}$  level of  $0.16 \pm 0.03$  pM was measured.

### Application of the labile $\text{Cu}^{2+}$ assay in a human cohort

In a cohort of 96 healthy human subjects, a mean labile serum  $\text{Cu}^{2+}$  level of  $0.14 \pm 0.05$  pM, ranging from 0.05 to 0.37 pM, was determined by the FP4-based assay (Fig. 5a). Previous studies based on a two-step method involving the removal of  $\text{Cu}^{2+}$  bound to CP and albumin by ultracentrifugation followed by instrumental quantification of  $\text{Cu}^{2+}$  in the eluate, reported  $\text{Cu}^{2+}$  concentrations in the nanomolar range<sup>6,22</sup>. However, this approach does not exclude the  $\text{Cu}^{2+}$  subset bound to other serum components, such as metallothionein or enzymes, and is therefore not comparable to the labile  $\text{Cu}^{2+}$  species determined by our direct fluorometric assay. Moreover, labile  $\text{Cu}^{2+}$  and total serum  $\text{Cu}^{2+}$  did not correlate (Fig. 5a), suggesting that labile  $\text{Cu}^{2+}$  is not simply a subset of the total copper pool, but reflects a discrete  $\text{Cu}^{2+}$  pool that is affected by other serum components. Another indication that labile free  $\text{Cu}^{2+}$  species is a separate pool from the total  $\text{Cu}^{2+}$  is the fact that it was possible to detect changes in free  $\text{Cu}^{2+}$  against the background of the CP-bound  $\text{Cu}^{2+}$  pool. Already the addition of a relatively small amount of  $\text{Cu}^{2+}$  to the human reference serum had a significant effect on the concentration of available labile  $\text{Cu}^{2+}$ , as spiking the reference serum (basal labile  $\text{Cu}^{2+}$  concentration of 0.05 pM) with only 20 nM  $\text{Cu}^{2+}$  resulted in a tripling of the labile  $\text{Cu}^{2+}$  level to  $0.15 \pm 0.02$  pM (Fig. 4d). Still, the vast majority of the added  $\text{Cu}^{2+}$  was not detected in the labile fraction, confirming an interaction with ligands able to buffer these ions to a significant extent. This shows that the labile  $\text{Cu}^{2+}$  determined in serum by our method not only depends on the amount of loosely bound (i.e., non-CP-bound)  $\text{Cu}^{2+}$ , but as well on the binding capacity of ligands with intermediate affinity.

In contrast to the significantly higher total serum  $\text{Cu}^{2+}$  concentration in sera of adult women than men (Fig. 5b), which has been well described in the literature<sup>41,42</sup>, labile  $\text{Cu}^{2+}$  levels did not differ significantly between female and male donors (Fig. 5c). Moreover, the labile  $\text{Cu}^{2+}$  species did not correlate with the age of donors (Fig. 5d). Correlation analysis of labile  $\text{Cu}^{2+}$  with total serum levels of selenium, iron or zinc did also not show any significant trend (Fig. 5e–g). In contrast, labile  $\text{Zn}^{2+}$  concentrations showed a weak negative correlation with labile  $\text{Cu}^{2+}$  levels in sera (Fig. 5h,  $r = -0.26$ ,  $p = 0.02$ ), which was not observed for total zinc and total copper levels in the same cohort (Fig. 5i).

### Labile $\text{Cu}^{2+}$ in Wilson’s disease

Finally, to assess the effect of a disease with copper dyshomeostasis on serum labile  $\text{Cu}^{2+}$ , the labile  $\text{Cu}^{2+}$  assay was applied to sera from 19 WD patients before and after initiation of medical therapy. As medications zinc, D-penicillamine, or trientine were used, which are commonly applied treatments for WD and supposed to reduce and revert the harmful copper accumulation during the disease<sup>43</sup>. Clinical parameters of the investigated human WD patients and the respective medical treatment are listed in Supplementary Tables 2 and 3. The

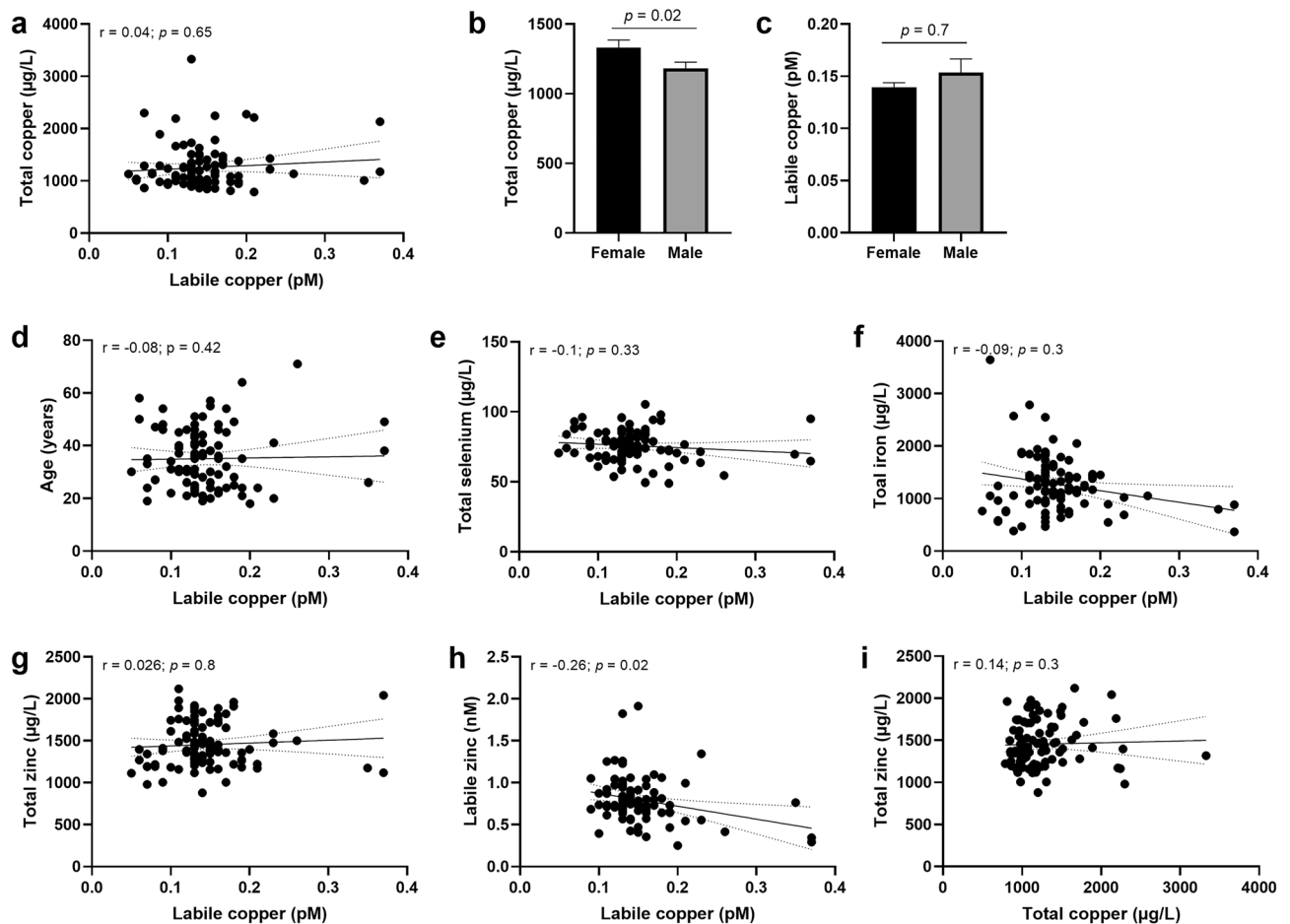


**Figure 5.** Labile  $\text{Cu}^{2+}$  in sera from a cohort of healthy human subjects. Labile  $\text{Cu}^{2+}$  shown in relation to total copper (a) in serum of a 'healthy' human cohort ( $N=96$ ). Sex differences in total copper of the serum are shown (b). Labile  $\text{Cu}^{2+}$  concentrations in the human cohort ( $N=96$ ) are depicted according to sex (c) and age of donors (d), total selenium (e) and iron levels (f) as well as to labile  $\text{Zn}^{2+}$  (g) and total zinc (h). Additionally, correlation of total zinc and total copper serum levels is shown (i). Data are presented as means + SD, and  $p$  values are indicated [non-parametric test using Mann–Whitney test (b,c)], and as scatter plots, including Spearman correlation coefficients ( $r$ ) and  $p$ -values.

average labile  $\text{Cu}^{2+}$  level in serum of WD patients of  $0.16 \pm 0.08$  pM was significantly reduced to  $0.10 \pm 0.07$  pM labile  $\text{Cu}^{2+}$  under ongoing treatment (Fig. 6a). This is consistent with another study reporting decreased loosely bound copper levels upon treatment of WD<sup>8</sup>. Total serum  $\text{Cu}^{2+}$  only slightly decreased after medical treatment (Fig. 6b). Similar to the healthy control cohort (Fig. 5a), total copper and labile  $\text{Cu}^{2+}$  did not correlate (Fig. 6c). Likewise, CP and labile  $\text{Cu}^{2+}$  showed no association (Fig. 6d), while total copper and CP showed a strong correlation ( $r=0.89$ ,  $p<0.001$ ) as described before (Fig. 6e)<sup>8</sup>. During WD the incorporation of  $\text{Cu}^{2+}$  in apo-CP in hepatocytes is impaired due to loss of function of ATPase copper transporting beta (ATP7B), responsible for shuttling absorbed  $\text{Cu}^{2+}$  into the Golgi. Consequently, serum CP and CP-bound  $\text{Cu}^{2+}$  levels in serum are low whereas non-CP bound  $\text{Cu}^{2+}$  is still excreted into the blood stream, resulting in an increase of loosely bound and labile  $\text{Cu}^{2+}$  in serum. Accordingly, serum  $\text{Cu}^{2+}$  species are suggested to represent the harmful  $\text{Cu}^{2+}$  serum pool leading to neurological disorders observed in WD, whereas total copper seems to be a poor marker of disease severity<sup>44</sup>. Increased loosely bound<sup>8,20</sup> or exchangeable  $\text{Cu}^{2+45}$  levels in serum of WD patients compared to healthy controls were reported before, suggesting it to be a more specific biomarker for disease diagnosis, status, or monitoring therapy success<sup>8,9,45</sup>. This is also consistent with the observations with the present fluorometric assay. The analysis of labile  $\text{Cu}^{2+}$  with this method could be used in the future to monitor the progress of medical therapy more easily. Its use for this purpose will need to be further validated in future studies with a range of different therapies for WD.

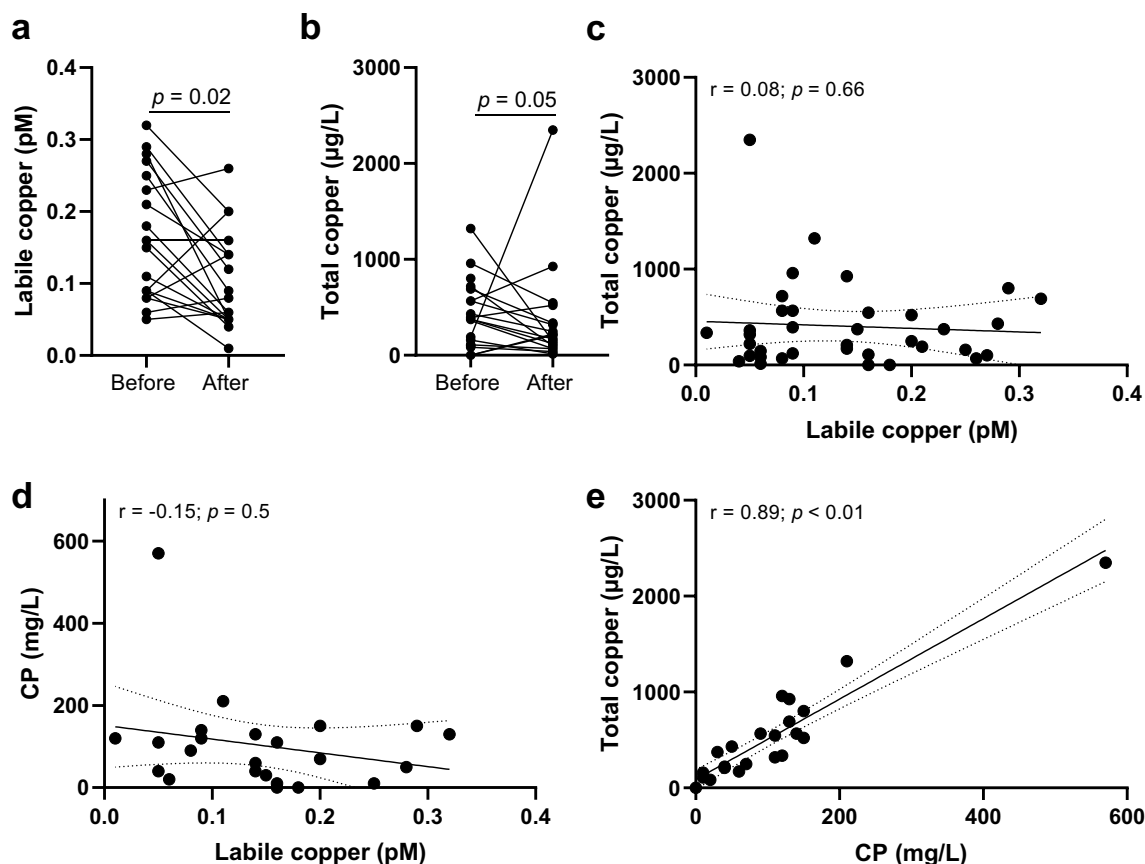


**Figure 6.** Labile  $\text{Cu}^{2+}$  in Wilson's disease patients before and after therapy. Labile  $\text{Cu}^{2+}$  (a) and total copper (b) concentrations in serum of a group of WD patients ( $N = 19$ ) before and after medical therapy. Labile  $\text{Cu}^{2+}$  concentrations in serum were compared to total copper (c) and ceruloplasmin levels (d) before and after therapy. Correlation of total copper and ceruloplasmin concentrations in serum of patients before and after treatment (e). Data are presented as means  $\pm$  SD, and  $p$  values are indicated (unpaired t-test (a,b)) and as scatter plots, including Spearman correlation coefficients ( $r$ ) and  $p$ -values (c–e).

## Conclusion

This study presents a newly developed direct fluorometric assay based on a novel  $\text{Cu}^{2+}$ -binding fluorescent probe. The high-throughput assay requires only 5  $\mu\text{l}$  of serum to quantify labile  $\text{Cu}^{2+}$  content in serum and can measure 76 serum samples in less than 4 h, making it a suitable platform for determining the labile  $\text{Cu}^{2+}$  concentration in serum samples from larger cohorts. Therefore, the assay may be used for future clinical applications, such as monitoring the copper status of WD patients during treatment. Furthermore, this study shows that the labile  $\text{Cu}^{2+}$  species most likely represents a separate serum  $\text{Cu}^{2+}$  pool and not just a subfraction of total serum  $\text{Cu}^{2+}$ . Future studies should further investigate the role of this highly available  $\text{Cu}^{2+}$  pool in the development and severity of diseases with impaired  $\text{Cu}^{2+}$  homeostasis.

## Data availability

The datasets generated during the current study are available from the corresponding author on reasonable request.

Received: 19 April 2023; Accepted: 31 July 2023

Published online: 07 August 2023

## References

- Sensi, S. L., Granzotto, A., Siotto, M. & Squitti, R. Copper and zinc dysregulation in Alzheimer's disease. *Trends Pharmacol. Sci.* **39**, 1049–1063. <https://doi.org/10.1016/j.tips.2018.10.001> (2018).
- Bornhorst, J., Kipp, A. P., Haase, H., Meyer, S. & Schwerdtle, T. The crux of inept biomarkers for risks and benefits of trace elements. *TrAC Trends Anal. Chem.* **104**, 183–190. <https://doi.org/10.1016/j.trac.2017.11.007> (2018).
- Linder, M. C. Ceruloplasmin and other copper binding components of blood plasma and their functions: An update. *Metallomics Integr. Biomet. Sci.* **8**, 887–905. <https://doi.org/10.1039/c6mt00103c> (2016).
- Kirsipuu, T. *et al.* Copper(II)-binding equilibria in human blood. *Sci. Rep.* **10**, 5686. <https://doi.org/10.1038/s41598-020-62560-4> (2020).
- Gioilli, B. D. *et al.* Secretion and uptake of copper via a small copper carrier in blood fluid. *Metallomics Integr. Biomet. Sci.* <https://doi.org/10.1093/mtomcs/mfac006> (2022).



6. Catalani, S. *et al.* Free copper in serum: An analytical challenge and its possible applications. *J. Trace Elem. Med. Biol. Organ Soc. Miner. Trace Elem.* **45**, 176–180. <https://doi.org/10.1016/j.jtemb.2017.11.006> (2018).
7. Witt, B., Schaumlöffel, D. & Schwerdtle, T. Subcellular localization of copper-cellular bioimaging with focus on neurological disorders. *Int. J. Mol. Sci.* <https://doi.org/10.3390/ijms21072341> (2020).
8. McMillin, G. A., Travis, J. J. & Hunt, J. W. Direct measurement of free copper in serum or plasma ultrafiltrate. *Am. J. Clin. Pathol.* **131**, 160–165. <https://doi.org/10.1309/ajcp7z9kbfvngyf> (2009).
9. Poujois, A. *et al.* Exchangeable copper: A reflection of the neurological severity in Wilson's disease. *Eur. J. Neurol.* **24**, 154–160. <https://doi.org/10.1111/ene.13171> (2017).
10. Ge, E. J. *et al.* Connecting copper and cancer: From transition metal signalling to metalloplasia. *Nat. Rev. Cancer* **22**, 102–113. <https://doi.org/10.1038/s41568-021-00417-2> (2022).
11. Squitti, R. *et al.* Meta-analysis of serum non-ceruloplasmin copper in Alzheimer's disease. *J. Alzheimers Dis.* **38**, 809–822. <https://doi.org/10.3233/JAD-131247> (2014).
12. Squitti, R. *et al.* Non-ceruloplasmin copper distinct subtypes in Alzheimer's disease: A genetic study of ATP7B frequency. *Mol. Neurobiol.* **54**, 671–681. <https://doi.org/10.1007/s12035-015-9664-6> (2017).
13. Squitti, R., Siotto, M., Cassetta, E., El Idrissi Imane, G. & Colabufo Nicola, A. *Clinical Chemistry and Laboratory Medicine (CCLM)*. Vol. 55. 1360 (2017).
14. Kumar, A., Sharma, P., Prasad, R. & Pal, A. An urgent need to assess safe levels of inorganic copper in nutritional supplements/parenteral nutrition for subset of Alzheimer's disease patients. *Neurotoxicology* **73**, 168–174. <https://doi.org/10.1016/j.neuro.2019.04.001> (2019).
15. Squitti, R. *et al.* Non-ceruloplasmin copper identifies a subtype of Alzheimer's disease (CuAD): Characterization of the cognitive profile and case of a CuAD patient carrying an RGS7 stop-loss variant. *Int. J. Mol. Sci.* <https://doi.org/10.3390/ijms24076377> (2023).
16. Kumar, A., Gupta, S., Sharma, P., Prasad, R. & Pal, A. In silico method for identification of novel copper and iron metabolism proteins in various neurodegenerative disorders. *Neurotoxicology* **73**, 50–57. <https://doi.org/10.1016/j.neuro.2019.02.020> (2019).
17. Walshe, J. M. Wilson's disease: The importance of measuring serum caeruloplasmin non-immunologically. *Ann. Clin. Biochem.* **40**, 115–121. <https://doi.org/10.1258/000456303763046021> (2003).
18. Twomey, P. J., Viljoen, A., House, I. M., Reynolds, T. M. & Wierzbicki, A. S. Relationship between serum copper, ceruloplasmin, and non-ceruloplasmin-bound copper in routine clinical practice. *Clin. Chem.* **51**, 1558–1559. <https://doi.org/10.1373/clinchem.2005.052688> (2005).
19. Quarles, C. D. *et al.* LC-ICP-MS method for the determination of “extractable copper” in serum. *Metallomics Integr. Biomet. Sci.* **12**, 1348–1355. <https://doi.org/10.1039/D0MT00132E> (2020).
20. del Castillo Busto, M. E., Cuello-Nunez, S., Ward-Deitrich, C., Morley, T. & Goenaga-Infante, H. A fit-for-purpose copper speciation method for the determination of exchangeable copper relevant to Wilson's disease. *Anal. Bioanal. Chem.* <https://doi.org/10.1007/s00216-021-03517-y> (2021).
21. Tuchtenhagen, M., Stiboller, M., Witt, B. & Schwerdtle, T. A novel approach for the determination of exchangeable copper in serum using protein precipitation. *J. Anal. At. Spectrom.* <https://doi.org/10.1039/D2JA00355D> (2023).
22. Inagaki, K. *et al.* Speciation of protein-binding zinc and copper in human blood serum by chelating resin pre-treatment and inductively coupled plasma mass spectrometry. *Analyst* **125**, 197–203. <https://doi.org/10.1039/a907088e> (2000).
23. Venelinov, T. I., Davies, I. M. & Beattie, J. H. Dialysis-Chelex method for determination of exchangeable copper in human plasma. *Anal. Bioanal. Chem.* **379**, 777–780. <https://doi.org/10.1007/s00216-004-2529-x> (2004).
24. Bohrer, D. *et al.* Comparison of ultrafiltration and solid phase extraction for the separation of free and protein-bound serum copper for the Wilson's disease diagnosis. *Clin. Chim. Acta Int. J. Clin. Chem.* **345**, 113–121. <https://doi.org/10.1016/j.cccn.2004.03.001> (2004).
25. El Balkhi, S. *et al.* Determination of ultrafiltrable and exchangeable copper in plasma: Stability and reference values in healthy subjects. *Anal. Bioanal. Chem.* **394**, 1477–1484. <https://doi.org/10.1007/s00216-009-2809-6> (2009).
26. Alker, W., Schwerdtle, T., Schomburg, L. & Haase, H. A zinpyr-1-based fluorimetric microassay for free zinc in human serum. *Int. J. Mol. Sci.* <https://doi.org/10.3390/ijms20164006> (2019).
27. Williamson, D. J., Fascione, M. A., Webb, M. E. & Turnbull, W. B. Efficient n-terminal labeling of proteins by use of sortase. *Angew. Chem. Int. Ed.* **51**, 9377–9380. <https://doi.org/10.1002/anie.201204538> (2012).
28. Young, T. R. *et al.* A set of robust fluorescent peptide probes for quantification of Cu(II) binding affinities in the micromolar to femtomolar range. *Metallomics Integr. Biomet. Sci.* **7**, 567–578. <https://doi.org/10.1039/c4mt00301b> (2015).
29. Xiao, Z. & Wedd, A. G. The challenges of determining metal–protein affinities. *Nat. Prod. Rep.* **27**, 768–789. <https://doi.org/10.1039/B906690j> (2010).
30. Sokolowska, M. & Bal, W. Cu(II) complexation by “non-coordinating” N-2-hydroxyethylpiperazine-N'-2-ethanesulfonic acid (HEPES buffer). *J. Inorg. Biochem.* **99**, 1653–1660. <https://doi.org/10.1016/j.jinorgbio.2005.05.007> (2005).
31. Einer, C. *et al.* A high-calorie diet aggravates mitochondrial dysfunction and triggers severe liver damage in Wilson disease rats. *Cell. Mol. Gastroenterol. Hepatol.* **7**, 571–596. <https://doi.org/10.1016/j.jcmgh.2018.12.005> (2019).
32. Grynkiewicz, G., Poenie, M. & Tsien, R. Y. A new generation of Ca<sup>2+</sup> indicators with greatly improved fluorescence properties. *J. Biol. Chem.* **260**, 3440–3450 (1985).
33. Heller, R. A. *et al.* Prediction of survival odds in COVID-19 by zinc, age and selenoprotein P as composite biomarker. *Redox Biol.* **38**, 101764. <https://doi.org/10.1016/j.redox.2020.101764> (2021).
34. Maeres, M. *et al.* Free zinc as a predictive marker for COVID-19 mortality risk. *Nutrients* **14**, 1407. <https://doi.org/10.3390/nu14071407> (2022).
35. Carter, K. P., Young, A. M. & Palmer, A. E. Fluorescent sensors for measuring metal ions in living systems. *Chem. Rev.* **114**, 4564–4601. <https://doi.org/10.1021/cr400546e> (2014).
36. Lichtman, J. W. & Conchello, J. A. Fluorescence microscopy. *Nat. Methods* **2**, 910–919. <https://doi.org/10.1038/nmeth817> (2005).
37. Lakowicz, J. R. *Principles of Fluorescence Spectroscopy* (Springer, 2006).
38. Bocca, B. *et al.* Nickel quantification in serum by a validated sector-field inductively coupled plasma mass spectrometry method: Assessment of tentative reference values for an Italian population. *Rapid Commun. Mass Spectrom.* **20**, 3289–3294. <https://doi.org/10.1002/rcm.2731> (2006).
39. Krezel, A. & Maret, W. Zinc-buffering capacity of a eukaryotic cell at physiological pZn. *J. Biol. Inorg. Chem.* **11**, 1049–1062. <https://doi.org/10.1007/s00775-006-0150-5> (2006).
40. Dineley, K. E., Malaiyandi, L. M. & Reynolds, I. J. A reevaluation of neuronal zinc measurements: Artifacts associated with high intracellular dye concentration. *Mol. Pharmacol.* **62**, 618–627. <https://doi.org/10.1124/mol.62.3.618> (2002).
41. Konz, T. *et al.* Sex-specific associations of blood-based nutrient profiling with body composition in the elderly. *Front. Physiol.* <https://doi.org/10.3389/fphys.2018.01935> (2019).
42. Piacenza, F. *et al.* Age, sex and BMI influence on copper, zinc and their major serum carrier proteins in a large European population including nonagenarian offspring from MARK-AGE study. *J. Gerontol. A Biol. Sci. Med. Sci.* <https://doi.org/10.1093/geron/56.11.134> (2021).
43. Mohr, I. & Weiss, K. H. Current anti-copper therapies in management of Wilson disease. *Ann. Transl. Med.* **7**, S69–S69. <https://doi.org/10.21037/atm.2019.02.48> (2019).

44. Stremmel, W. & Weiskirchen, R. Therapeutic strategies in Wilson disease: Pathophysiology and mode of action. *Ann. Transl. Med.* **9**, 732–732. <https://doi.org/10.21037/atm-20-3090> (2021).
45. El Balkhi, S. *et al.* Relative exchangeable copper: A new highly sensitive and highly specific biomarker for Wilson's disease diagnosis. *Clin. Chim. Acta Int. J. Clin. Chem.* **412**, 2254–2260. <https://doi.org/10.1016/j.cca.2011.08.019> (2011).

### Acknowledgements

This research was funded by the Deutsche Forschungsgemeinschaft (DFG), Research Unit FOR-2558 TraceAge-DFG Research Unit on Interactions of essential trace elements in healthy and diseased elderly, Potsdam-Berlin-Jena (HA 4318/4-2, Scho 849/6-2). M.M. is funded by DFG (MA 9681/1-1). M.K.-K. is funded by the Dahlem Research School (Elsa-Neumann-Stipendium für Promovierende, T70011).

### Author contributions

Conception of the study: M.M., H.H.; analysis: A.H., C.S., M.K.-K., J.H., M.M., I. M.; interpretation of data: M.M., H.H., resources: H.H., L.S., H.Z., R.D.S., U.M. writing—original draft: M.M., M.K.-K.; writing—review and editing: H.H., C.K., I.M., L.S., H.Z., R.D.S., U.M.

### Funding

Open Access funding enabled and organized by Projekt DEAL.

### Competing interests

The authors declare no competing interests.

### Additional information

**Supplementary Information** The online version contains supplementary material available at <https://doi.org/10.1038/s41598-023-39841-9>.

**Correspondence** and requests for materials should be addressed to H.H.

**Reprints and permissions information** is available at [www.nature.com/reprints](http://www.nature.com/reprints).

**Publisher's note** Springer Nature remains neutral with regard to jurisdictional claims in published maps and institutional affiliations.



**Open Access** This article is licensed under a Creative Commons Attribution 4.0 International License, which permits use, sharing, adaptation, distribution and reproduction in any medium or format, as long as you give appropriate credit to the original author(s) and the source, provide a link to the Creative Commons licence, and indicate if changes were made. The images or other third party material in this article are included in the article's Creative Commons licence, unless indicated otherwise in a credit line to the material. If material is not included in the article's Creative Commons licence and your intended use is not permitted by statutory regulation or exceeds the permitted use, you will need to obtain permission directly from the copyright holder. To view a copy of this licence, visit <http://creativecommons.org/licenses/by/4.0/>.

© The Author(s) 2023, corrected publication 2024